Adsorption (2012) 18:251–263
DOI 10.1007/s10450-012-9398-y

A dynamic column breakthrough apparatus for adsorption capacity measurements with quantitative uncertainties

Paul S. Hofman · Thomas E. Rufford · K. Ida Chan · Eric F. May

Received: 1 December 2011 / Accepted: 13 August 2012 / Published online: 31 August 2012

Abstract A dynamic column breakthrough (DCB) apparatus was used to study the separation of $CH_4 + N_2$ gas mixtures using two zeolites, H^+-mordenite and 13X, at temperatures of (229.2 and 301.9) K and pressures to 792.9 kPa. The apparatus is not limited to the study of dilute adsorbates within inert carrier gases because the instrumentation allows the effluent flow rate to be measured accurately: a method for correcting apparent effluent mass flow readings for large changes in effluent composition is described. The mathematical framework used to determine equilibrium adsorption capacities from the dynamic adsorption experiments is presented and includes a method for estimating quantitatively the uncertainties of the measured capacities. Dynamic adsorption experiments were conducted with pure CH_4, pure N_2 and equimolar $CH_4 + N_2$ mixtures, and the results were compared with similar static adsorption experiments reported in the literature. The 13X zeolite had the greater adsorption capacity for both CH_4 and N_2. At 792 kPa the equilibrium capacities of the 13X zeolite increased from 2.13 ± 0.14 mmol g^{-1} for CH_4 and 1.36 ± 0.10 mmol g^{-1} for N_2 at 301.9 K to 3.97 ± 0.19 mmol g^{-1} for CH_4 and 3.33 ± 0.12 mmol g^{-1} for N_2 at 229.2 K. Both zeolites preferentially adsorbed CH_4; however, the mordenite had a greater equilibrium selectivity of 3.5 ± 0.4 at 301.9 K. Equilibrium selectivities inferred from pure fluid capacities using the Ideal Adsorbed Solution theory were limited by the accuracy of the literature pure fluid Toth models. Equilibrium capacities with quantitative uncertainties derived directly from DCB measurements without reference to a dynamic model should help increase the accuracy of mass transfer parameters extracted by the regression of such models to time dependent data.

Keywords Adsorption · Zeolites · Packed bed · Pressure swing adsorption · Petroleum · Gases

1 Introduction

The separation and purification of gas mixtures by pressure swing adsorption (PSA) is an established industrial separation technology used, for example, in the separation of air into oxygen and nitrogen, the production of hydrogen, and the capture of volatile organic compounds from waste gas streams (Sircar 2002; Campbell 1974; Kidnay and Parrish 2006; Yang 1987). The design of PSA systems requires several key input data: (1) adsorption equilibria, (2) mass-transfer characteristics and (3) enthalpies of adsorption. The three main experimental techniques used to produce such data are the volumetric, the gravimetric and the dynamic breakthrough (or flow) methods (Young and Crowell 1962; Yang 1987; Rouquerol et al. 1999; Ross and Olivier 1964; Ruthven 1984; Keller and Staudt 2010; Karger and Ruthven 1992; Do 1998; Broom 2011), which have been reviewed and compared with other methods by several authors including Sircar (2006, 2007). The most common type of adsorption data reported in the literature are equilibrium adsorption capacities of pure gases made by static (volumetric or gravimetric) methods, largely because these are the easiest types of measurement to make and several commercial instruments are available to conduct them. However, while PSA systems can be based on pure fluid adsorption data

P.S. Hofman · T.E. Rufford · E.F. May (✉)
Centre for Energy, School of Mechanical & Chemical Engineering, The University of Western Australia, 35 Stirling Highway, Crawley WA 6009, Australia
e-mail: Eric.May@uwa.edu.au

K.I. Chan
Chevron Energy Technology Company, Houston, TX 77002, USA

measured by the static method, the design is often over-engineered to account for the critical differences between the conditions of the static experiments with pure fluids and the dynamic conditions of an industrial gas separation process. Economic analyses of PSA systems have shown that, over the life of a facility, a 2 % increase in product recovery can yield 150 % of the cost of the PSA plant itself in generated revenue (Sircar 2002, 2006). Thus, representative dynamic adsorption data for gas mixtures are particularly valuable to the development of PSA processes with reduced design margins.

The dynamic column breakthrough (DCB) method provides a laboratory-based adsorption experiment that can more closely match the conditions in an industrial-scale gas separation process than achievable with static adsorption experiments (Rajendran et al. 2008). Consequently, the data produced with the DCB method improve the prospects for reliable scale-up of the adsorption technology (Guntuka et al. 2008). However, although experiments have been made using variations of the DCB method for over 60 years (Habgood 1958; Delgado et al. 2006b; Grande et al. 2003; Malek and Farooq 1996; Farooq and Ruthven 1990; Tezel et al. 1992), it has been most commonly applied through experiments involving the pulsed injection of dilute adsorbates into an inert carrier gas passing through a column packed with the adsorbent. This may in part be due to the difficulties associated with the measurement of the flow rate of effluent from the packed-column during a DCB experiment with high adsorbate concentrations in the feed gas. In such an experiment, both the flow rate and composition of the effluent from the column vary significantly and, consequently, can be difficult to measure accurately: for example, flow meters that use thermal sensors to determine flow are very difficult to use reliably with mixtures of arbitrary and varying composition. The most common method of extending DCB experiments beyond studies of dilute adsorbates is through the application of a dynamic numerical model of the DCB experiment to estimate the effluent flow rate. Other key parameters such as mass and heat transfer coefficients are then generally estimated through regression of that model to the measured composition data. However, the adjustable parameters of such dynamic models are strongly correlated with each other which makes reliable estimation of their uncertainty very difficult, and means that during a regression the models can converge to inaccurate values of those parameters if there are too many degrees of freedom. Thus, when relying on dynamic models to describe the results of DCB experiments it is preferable to have independent information about the equilibrium adsorption capacities, which often requires an auxiliary set of measurements with a static apparatus. In this work we present an apparatus that enables adsorption capacities to be determined directly from DCB experiments at high adsorbate concentrations without reference to a dynamic model and, for the first time, a method to estimate robustly the uncertainties in the measured capacities.

Several recent papers have reported apparatus with instrumentation that allows the effluent flow rate to be monitored and used to test the predictions of dynamic models (Guntuka et al. 2008; Mulgundmath et al. 2012; Lopes et al. 2011; Casas et al. 2012; Won et al. 2012). However, an important detail relating to the flow measurement has not been covered in these papers: the correction of the meter's reading to account for variation in the effluent composition. Several different operating principles are used by various commercially-available flow meters; however, all flow meters require knowledge of one or more thermophysical properties of the fluid being measured, such as viscosity and/or density, to convert the measured quantity (pressure drop in an orifice meter, resonance period in a coriolis meter) to a flow rate. Since such thermophysical properties depend sensitively on fluid composition, flow meters are generally 'calibrated' to operate with a specific pure fluid. It is possible to use the flow meter accurately with a different pure fluid, or even a mixture of known composition, provided the appropriate thermophysical properties of the fluid can be calculated *and* if the model relating the measured quantity to the flow rate is sufficiently well known. Of the five recent papers that incorporated an effluent flow meter, only Guntuka et al. (2008) and Mulgundmath et al. (2012) reported the model or type of flow meter used, and none of the papers detail how the effluent composition was used to correct the meter's raw flow reading. In this work we describe a method for obtaining accurate effluent flow measurements during DCB experiments with mixtures containing concentrated adsorbates by using an orifice-type flow meter and the measured effluent composition.

The particular motivation for this work is the development of PSA processes for separating the mixtures of N_2 and CH_4 present at various stages in the cryogenic plants used to produce liquefied natural gas (LNG). Adsorption-based processes for separating mixtures of CH_4 and N_2 in natural gas processing have the potential for lower energy requirements, smaller plant foot-prints and lower capital costs than the conventional cryogenic distillation technologies. Commercial PSA-based separations of N_2 and CH_4 are already utilized within the natural gas industry using various adsorbents (American Energies Pipeline 2009; Tucker Gas Processing Equipment Inc. 2011; Sep-Pro Systems Inc. 2009; Kuznicki et al. 2001; Ruthven 2011), although currently they are limited to treating feed gas flow rates of up to 15 million standard cubic feet per day ($=5.08\ Nm^3/s$) (Mitariten 2009). There are several promising avenues which may lead to the further deployment of PSA processes for separating N_2 from CH_4, particularly in LNG plants, including: (i) the ready accessibility of low temperatures and high-pressures within the plant; (ii) the need, prior to disposal, to

upgrade or purify N_2- or CH_4-dominant streams which are a by-product of LNG production; and (iii) the wide range of existing commercial adsorbents and/or newly developed adsorbents which have not been adequately tested for this application.

In this paper we demonstrate how a DCB apparatus with appropriate instrumentation can be used to determine accurately equilibrium adsorption capacities for pure fluids and gas mixtures over a wide range of conditions, including those conditions relevant to the separation of N_2 and CH_4 mixtures found at various points in LNG plants. Measurements are reported for two commercially available zeolites over the range (229.2 to 301.9) K and (104.0 to 792.9) kPa using concentrated adsorbates. Importantly, we present a quantitative method to estimate the uncertainties of those adsorption capacities, which to our knowledge has not been reported elsewhere. Such equilibrium data and their uncertainty estimates are crucial to both adsorption science and engineering (Valenzuela and Myers 1989; Al-Muhtaseb 2010; Sircar 2002) yet their acquisition with static methods is generally quite challenging for gas mixtures. In a subsequent paper, we will apply and extend existing dynamic adsorption models to further analyse the time-dependent adsorption data from this DCB apparatus, with the objectives of determining the mass and heat transfer parameters relevant to the design of PSA systems.

2 Apparatus and materials

A schematic of the DCB apparatus is shown in Fig. 1. The adsorption column (a 130 mm long by 22.2 mm inner diameter stainless steel tube) and an inlet cooling loop (ICL) were located inside a stirred air bath, equipped with a liquid nitrogen spray cooling system. This thermally controlled zone was capable of producing temperatures between 190 K and 498 K. The loop of $1/8''$ tubing that formed the ICL was thermally anchored to a copper spool to ensure the feed gas entering the column was in thermal equilibrium with the adsorption column. An outlet heating loop (OHL) was installed at the column's outlet to heat the effluent gas back to ambient temperature and thus ensure accurate readings at the back-pressure regulator (BPR-2), outlet flow meter (MFM), and mass spectrometer (MS). The adsorbent bed temperature was monitored at three positions along the length of the column with 100 Ω platinum resistance thermometers (T-1, T-2 and T-3 at 32.7 mm, 65.4 mm and 98.1 mm from the column entrance, respectively). These thermometers were calibrated to ITS-90 over the range 77–313 K with an uncertainty of 0.2 K.

The flow rate and composition of gas mixtures (including pure gases) to the column was regulated by four mass flow controllers (MFC-1 to MFC-4). The full scale of each mass flow controller was 136 μmol s^{-1} (200 standard cm^3 min^{-1} [sccm]) with an uncertainty on the flow measurement of 0.8 % of the reading plus 0.2 % of full scale, as stated by

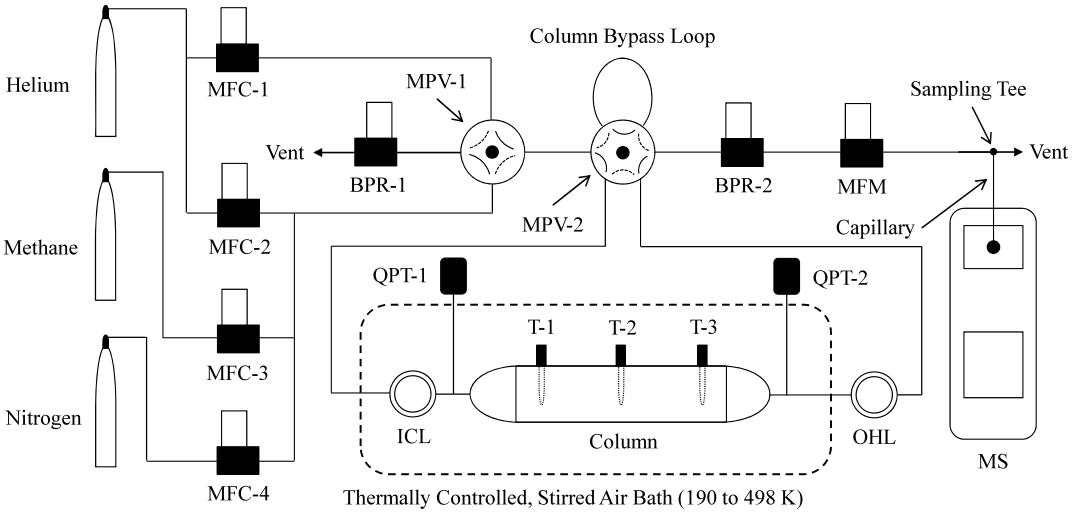

MFC – Mass Flow Controller
BPR – Back Pressure Regulator
MPV – Multi-position Valve
ICL – Inlet Cooling Loop
OHL – Outlet Heating Loop
MFM – Mass Flow Meter
MS – Mass Spectrometer
QPT – Quartz-crystal Pressure Transducer
T – Platinum Resistance Thermometer

Fig. 1 Schematic diagram of the dynamic column breakthrough (DCB) apparatus

the manufacturer and confirmed by gravimetric flow calibrations performed in our laboratory. The column outlet flow was measured by a mass flow meter (MFM), with the same full scale and uncertainty as the MFCs. A zero-dead-volume multi-position valve (MPV-1) was used to switch the column feed gas between helium and the pure or mixed gas feed (N_2, CH_4 and He). A second zero-dead-volume multi-position valve (MPV-2) allowed the column containing the adsorbent to be bypassed.

Adsorption experiments were performed with constant column outlet pressures from 104.0 kPa to 792.9 kPa, controlled by BPR-2. Another back-pressure regulator (BPR-1) was used at the vent of MPV-1 to prevent back-flow from the column whenever MPV-1 was actuated. The pressures at the inlet and outlet of the column were measured by independent quartz-crystal pressure transducers (QPT-1 and QPT-2), each with a full scale of 1380 kPa and a specified uncertainty over this range of 0.1 kPa.

The column effluent composition was measured using a mass spectrometer (MS, Stanford Research Systems QMS-100) through a sample capillary attached to a tee on the main flow line from the MFM. This tee configuration (1) ensured that the MFM always operated at atmospheric pressure, which decreased the need for pressure corrections of the MFM reading and (2) controlled the sample flow to the MS within the range of 1–2 $\mu mol\,s^{-1}$ (as well as protecting the MS from overpressure) when the outlet flow from the column varied from 4–136 $\mu mol\,s^{-1}$. The MS had a mass range of 0 to 100 atomic mass units, a manufacturer-specified composition uncertainty of 1 % by mole and a response time of less than 0.2 s (once gas entered the inlet of the MS). The uncertainty in the composition measurement was verified by preparing gas mixtures by varying the ratio of flows of He, CH_4 and N_2 through MFC-2, MFC-3 and MFC-4 via the column bypass direct to the MS. Further testing was performed by flowing a gravimetrically prepared mixture of $0.505N_2 + 0.495CH_4$ through the MS. The gas mixture was supplied by BOC and had an estimated uncertainty of 0.2 % by mole.

The volume of each section of the apparatus outside the column was estimated using three independent methods: gravimetric, dimensional and residence time. The results of these measurements are shown in Table 1. Conical adapter sections were used to connect the tubing (ID $\approx$ 2.5 mm) to the 22.5 mm ID column, and consisted of about half of the extra-column volume. The gravimetric and residence time measurements were performed with the column removed and the inlet and outlet cones connected together. The dimensional measurements were made by disassembling a duplicate BPR and MFM to determine their internal dimensions. Further details of these volume measurements are given by Hofman (2012). Importantly, the volumes determined by all three methods were consistent within their combined uncertainties.

Table 1 Estimation of extra-column void volumes (at standard conditions) in the dynamic column breakthrough apparatus

Section/Component	Method	Volume [cm^3]
Inlet tube (from MPV-1)	Dimensional	5.3
Inlet cone		8.4
Outlet cone		8.4
High-pressure outlet tube (to BPR-2)		8.0
Low-pressure outlet tube (from BPR-2 to MS)		3.0
Total	Dimensional	33.1 ± 0.6
Total	Gravimetric	38.3 ± 2.9
Total	Residence time	36.0 ± 3.0

In this DCB apparatus the effluent mass flow meter MFM used was of the orifice-plate type in which a pressure drop measured across a unique internal restriction, known as a laminar flow element, is used to determine the mass flow rate from an assumed gas viscosity. The flow of effluent gas mixtures can be determined with this type of meter by correcting the apparent flow rate by the ratio of the mixture viscosity to that of the assumed gas viscosity if the composition of the effluent gas mixture is known. The MFM used was factory-calibrated for He and operated in "He mode" so that the apparent flow rate corresponded to that for a gas with the viscosity of He. Then, the MS measurements of the effluent composition were used to determine the ratio of the He viscosity to that of the gas mixture's using an empirical correlation

$$\frac{\eta_{He}}{\eta_{mix}} = \sum_i \frac{y_i \frac{\eta_{He}}{\eta_i}}{y_i + \sum_{j \neq i} (a_{ij} y_j + b_{ij} y_j^2)}. \quad (1)$$

Here, y_i is the mole fraction of component i, η_i is the viscosity of pure component i and the a_{ij} and b_{ij} are empirical parameters determined from calibration experiments. The functional form of Eq. (1) is based on the gas mixture viscosity correlation described by Assael et al. (1996); however, it was necessary to extend the correlation to achieve an adequate representation of viscosity ratios over a wide range of compositions. The empirical parameters a_{ij} and b_{ij} for CH_4, N_2 and He were determined by regression of the effluent flow rate (measured by the MFM and corrected by Eq. (1)) to force agreement with the inlet mixture flow rate set using MFC-2, MFC-3 and MFC-4 and the column bypass loop. (These flow calibration experiments with mixtures also allowed the uncertainty of composition measurements made with the MS to be checked.) In total 304 experiments with pure, binary and ternary mixtures of CH_4, N_2 and He were conducted resulting in 12 empirical parameters determined by a least squares regression. It is important to

note that Eq. (1) was only used for the purpose of interpolating viscosity ratios as a function of composition and that the parameters a_{ij} and b_{ij} are not general in nature. The time delay between the MFM and the MS had a negligible effect on the efficacy of the viscosity ratio correction because of the small tube volume between these instruments (<0.3 cm^3) and the fast response time of the MS. The combined uncertainties of the viscosity ratio correlation and the MS composition measurement resulted in the estimated uncertainty of the MFM reading for mixtures increasing to 1.6 % of the reading + 0.2 % of full scale.

A fully automated data acquisition and control system implemented in LabVIEW 8.2.1 (LabVIEW 2007) was used to actuate the valves, write the set points for the MFCs and BPRs, and monitor and record readings from all of the instruments. The measured mass flows and compositions were sampled once a second, while column residence times typically ranged from 10 to 1000 s. These two time scales are critical to the full analysis of the dynamic data. The thermometers monitoring the internal bed temperature along the column and the pressure transducers (QPT-1, QPT-2) were also sampled once a second.

All gases used in this work were supplied by BOC who stated the following fractional purities: He 99.999 %, CH_4 99.995 %, and N_2 99.999 %. The estimated uncertainty of the adsorption measurements due to gas purity was assumed to be negligible. The adsorbents used to demonstrate the operation of this system were a synthetic H^+-mordenite HSZ-640HOA provided by TOSOH Corporation (Japan) and a synthetic 13X zeolite provided by Shanghai MLC (China). Adsorbents were regenerated in a separate vessel under vacuum (10 Pa) at 573 K for 24 h, and the regeneration vessel was backfilled with N_2 before loading into the adsorption column. The mass of the regenerated mordenite and 13X samples used in the adsorption experiments were (29.036 ± 0.005) and (26.455 ± 0.005) g, respectively.

3 Method and analysis

The regenerated adsorbent was loaded into the column quickly to minimize the exposure of the (N_2-saturated) adsorbent to the air. A 20 µm filter washer was fitted at the outlet end of the column, and the regenerated adsorbent was poured into the (inverted) column. The column was tapped gently to settle the pellets in the bed and around the three bed thermometers (the sensors remained in place during the loading). The packed column was then sealed with a second 20 µm filter washer fitted at the inlet and connected to the ICL and OHL (and pressure transducers) inside the oven. Before each adsorption experiment, the adsorbent was degassed *in situ* with a 136 µmol s^{-1} flow of He for a minimum of 3 h at 301.7 K. Complete degassing was assumed when

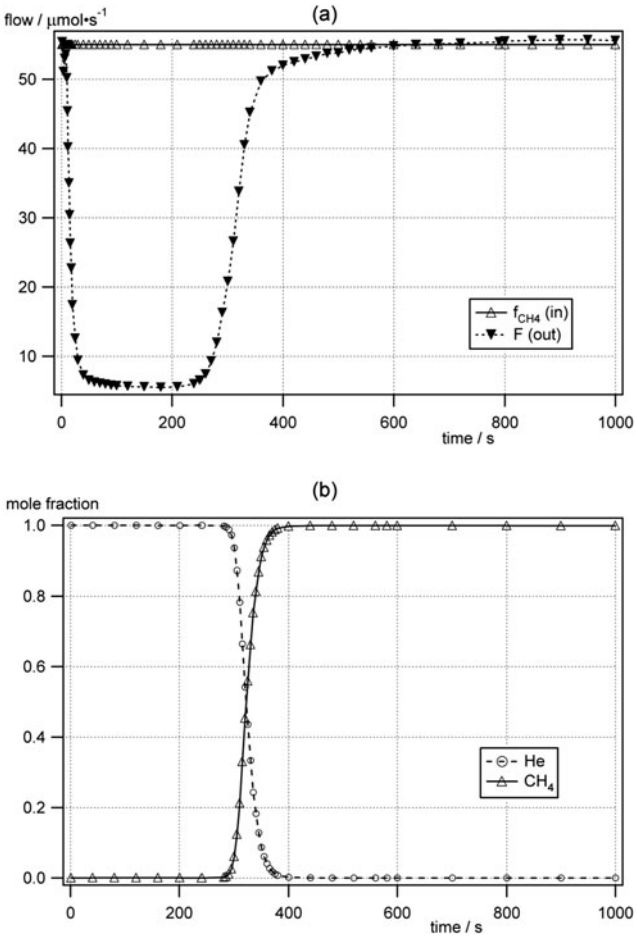

Fig. 2 Dynamic breakthrough profile for the adsorption of CH_4 on mordenite at 104 kPa, 301.9 K. (**a**) Column feed and effluent flow rates. (**b**) Effluent mole fraction compositions

the effluent composition was measured to be >99.99 % He by mole with the total flow reduced to 17 µmol s^{-1}. The reduced flow increased the fraction of any species in the effluent still desorbing and improved the ability to resolve whether the rate of desorption had reached a sufficiently low level.

Once the adsorbent was degassed, the first step in the adsorption experiment was to actuate MPV-2 to bypass the column and to set BPR-1 and BPR-2 to the required pressures. The feed gas mixture was prepared using MFC-2, MFC-3 and MFC-4. Then MPV-1 was actuated to direct the feed gas flow through the bypass to the MFM and the MS. The flow and composition readings from these downstream instruments were recorded at the conditions at which the experiment was to be performed. These values were compared to the MFM and the MS readings at the conclusion of an adsorption experiment to verify the system had attained equilibrium. Generally a small offset was observed between the measured inlet and the effluent flow rates when the column was in the bypass mode and was evident in the raw data once the system had reached equilibrium (for example as shown

in Fig. 2a). This measurement offset was within the uncertainty of the mass flow instruments; nevertheless, the small difference was accounted for during the integration of the material balances described below by a normalization procedure. Any offset was eliminated during data analysis by multiplying all the effluent flow meter readings acquired during the adsorption measurement by the ratio of the apparent inlet and effluent flows obtained with the column bypassed. The standard deviation of the inlet to outlet flow ratios for the measurements was 0.017. Measurements made with the MFCs operating at pressures above 110 kPa usually resulted in larger offsets of up to 5 %.

Following the initial comparisons of the inlet and effluent instrumentation using the bypass loop, MPV-1 and MPV-2 were actuated to establish a flow of helium through the column and allow BPR-2 to reach its set point before the adsorption measurement commenced. Once the system had stabilized and a steady pressure gradient was observed along the column, the adsorption measurement was initiated by actuating MPV-2 to direct the feed gas mixture into the column. In a typical experiment, the feed gas took between (4 to 180) s to reach the adsorbent bed, depending on the column pressure and temperature, after MPV-2 was actuated and, once adsorption of feed gas components began, the change in effluent flow rate measured at the MFM was observed with virtually no delay. An example of the rapid change in effluent flow rate upon the feed gas reaching the column is shown in Fig. 2(a): the change in gas velocity due to adsorption at the start of the column propagated at the speed of sound to the MFM. As the adsorbent approached its saturation condition the total effluent flow rate increased and then approached the inlet flow rate asymptotically. At approximately this time, the composition breakthrough would be observed with the MS and, eventually, the outlet composition measured by the MS would become equal to the feed composition determined by the MFCs, as shown in Fig. 2(b). Depending on the average gas velocity through the column, the composition breakthrough front was detected at the MS about (6 to 600) seconds after exiting the outlet of the column.

Upon completion of the adsorption step, MPV-1 was switched so that helium from MFC-1 flowed into the column initiating the desorption process. Desorption data were collected from each experiment; however, only the adsorption data were used to calculate the equilibrium adsorption capacities because, as discussed by Guntuka et al. (2008), the variations in effluent flow rate and composition during desorption are near or below the detection limits of the respective instruments. This observation is consistent with the results of our uncertainty analysis below, which indicates that adsorption parameters determined from dynamic desorption experiments will have much larger uncertainties than those determined from adsorption experiments.

Equilibrium adsorption capacities and selectivities were derived from the experimental data through a material balance analysis:

$$moles\ in - moles\ out = accumulation \tag{2}$$

where

$$moles\ in = \int_{t'=t_0}^{t} f_i\,dt', \tag{3}$$

$$moles\ out = \int_{t'=t_0}^{t} F y_i\,dt', \tag{4}$$

$$\begin{aligned} accumulation &= \left[n_i^{(\mathrm{gas})} + n_i^{(\mathrm{ads})}\right]_t - \left[n_i^{(\mathrm{gas})} + n_i^{(\mathrm{ads})}\right]_{t_0} \\ &= [V_{\mathrm{gas}}\rho_i]_t - [V_{\mathrm{gas}}\rho_i]_{t_0} + m\,Q_{\mathrm{ex},i}(t). \end{aligned} \tag{5}$$

In Eqs. (2)–(4), f_i is the molar flow of component i into the column (determined by the MFCs), F is the total molar flow of effluent from the column (measured by the MFM), y_i is the mole fraction of component i at the MFM outlet (measured by the MS), and t_0 is the time at which the feed gas is directed into the column. In Eq. (5), $n_i^{(\mathrm{gas})}$ is the number of moles of component i in the gas phase within the DCB apparatus void volumes, $n_i^{(\mathrm{ads})}$ is the number of moles of component i in the adsorbed phase, V_{gas} is the volume in the column occupied by the gas phase, ρ_i is the molar density of component i in the gas phase, m is the mass of adsorbent, and $Q_{\mathrm{ex},i}$ is the excess adsorption capacity of component i in the adsorbed phase in moles per unit mass of adsorbent. At the start of the adsorption experiment it is assumed that the number of moles of component i adsorbed is zero ($Q_{\mathrm{ex},i}(t_0) = 0$). Substituting Eqs. (3)–(5) into (2) gives an expression valid at any time during the adsorption experiment:

$$\begin{aligned} \int_{t'=t_0}^{t} f_i\,dt' - \int_{t'=t_0}^{t} F y_i\,dt' &= \left(n_{i,t}^{(\mathrm{gas})} - n_{i,t_0}^{(\mathrm{gas})}\right) + m\,Q_{\mathrm{ex},i}(t) \\ &= \Delta n_i^{(\mathrm{gas})} + m\,Q_{\mathrm{ex},i}(t). \end{aligned} \tag{6}$$

The determination of equilibrium adsorption capacity from a breakthrough experiment requires several conditions to be met: (1) the feed and effluent flow rates and compositions should be equal and (2) the pressure and temperature along the adsorbent bed should be uniform and non-varying. Adsorption is an exothermic process, and in our experiments with an undiluted gas feed the heat released often resulted in temperature rises in the bed of more than several kelvin. Figure 3 shows the measured bed temperatures during an adsorption experiment conducted near ambient conditions. During the experiment it is apparent that the assumption that the system is isothermal is not valid, and the inclusion of an energy balance term in Eq. (6) would be necessary to more accurately describe the thermal effects of adsorption in a time dependent model. However, the bed temperatures ultimately returned to their initial conditions by the completion of the experiment (as shown in Fig. 3) and, therefore,

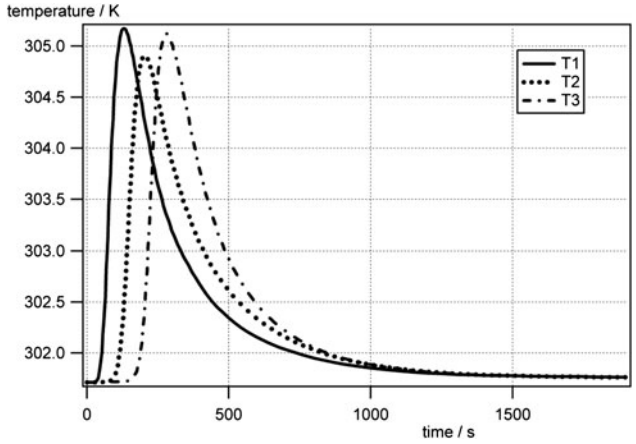

Fig. 3 Temperatures measured by the column thermometers T-1, T-2 and T-3 (see Fig. 1) during the dynamic adsorption of CH_4 on mordenite at 104 kPa, 301.9 K, corresponding to the data shown in Fig. 2

for the purpose of calculating equilibrium adsorption capacities, the assumption of isothermal behavior was justified. The bed temperature measurements were also used to reject data when this thermal condition was violated on occasion because of air-bath instability during the experiment.

Under the assumptions of constant pressure and ideal gas behavior, the component material balance in Eq. (6) is subject to the constraint $n_{\text{tot}}^{(\text{gas})} = \text{constant}$, where $n_{\text{tot}}^{(\text{gas})}$ is the total number of moles in the gas phase. Initially the bed is filled with helium and under the assumption that helium does not adsorb, which is justified at the temperatures and pressures of these experiments (Malbrunot et al. 1997). The change in the amount of helium in the gas phase once steady state is reached at t_{eq} is

$$\Delta n_{\text{He}}^{(\text{gas})} = \int_{t'=t_0}^{t_{\text{eq}}} f_{\text{He}} dt' - \int_{t'=t_0}^{t_{\text{eq}}} F y_{\text{He}} dt'. \tag{7}$$

The amount of gas phase helium in the DCB apparatus at the initial condition includes the helium in the internal pore spaces of the adsorbent pellets (pore volume or intraparticle volume), in the interparticle void volumes, and in the voids of the apparatus outside the packed column, which are listed in Table 1. Although the equilibrium adsorption capacities reported in this paper can be calculated directly from Eqs. (6)–(10) using the component flow rate data without the need to calculate void volumes directly, the determination of the void volumes of the DCB apparatus allows a consistency check to be conducted on the amount of helium displaced in each experiment. Furthermore, the accounting of the void volumes in the DCB apparatus is required for the kinetic analysis of the breakthrough curves, which will be reported in a later paper.

The helium in the gas phase is replaced with the other components in the gas phase:

$$\sum_{j \neq \text{He}} n_j^{(\text{gas})} = \Delta n_{\text{He}}^{(\text{gas})} \rightarrow n_j^{(\text{gas})} = y_j^* \Delta n_{\text{He}}^{(\text{gas})}. \tag{8}$$

Here y_j^* is gas phase mole fraction for component j once equilibrium has been reached, and the index j refers to any component other than He. Thus, at steady state the component material balance in Eq. (6) becomes

$$m Q_{\text{ex},j}^* = \int_{t'=t_0}^{t_{\text{eq}}} f_j dt' - \int_{t'=t_0}^{t_{\text{eq}}} F y_j dt' - y_j^* \left[\int_{t'=t_0}^{t_{\text{eq}}} f_{\text{He}} dt' - \int_{t'=t_0}^{t_{\text{eq}}} F y_{\text{He}} dt' \right], \tag{9}$$

where $Q_{\text{ex},j}^*$ is the excess adsorption capacity of component j at equilibrium. Summing Eq. (9) over all components leads to a statement of total material balance at steady state

$$m Q_{\text{ex,tot}}^* = \int_{t'=t_0}^{t_{\text{eq}}} (f - F) dt'. \tag{10}$$

Here $f = \sum_i f_i$ is the total molar flow into the column and $Q_{\text{ex,tot}}^*$ is the total number of moles adsorbed per unit mass of adsorbent. For a feed gas with a single adsorbate, Eq. (10) can be used to determine the excess adsorption capacity, without reference to the composition of the effluent flow.

To convert the excess adsorption capacity to the absolute adsorption capacity, $Q_{\text{abs},i}^*$, the density of the adsorbed phase mixture was estimated using an ideal mixing rule and predictions for the densities of the adsorbed phase for pure compounds. The densities of the pure adsorbed phases of CH_4 and N_2 were estimated to be 0.354 g cm^{-3} and 0.701 g cm^{-3}, respectively, using the Ono-Kondo model (Sudibandriyo et al. 2003). The molar density of the gas mixture was determined at the measured pressure, temperature and composition, from the GERG-2004 equation of state (Kunz et al. 2006) as implemented in the software REFPROP 8.0 (Lemmon et al. 2007).

Equation (9) represents the component material balance across the column in integral form and can only be used to determine equilibrium adsorption properties from dynamic column data once the system has reached steady state. To determine $Q_{\text{ex},i}(t)$ and extract the mass-transfer coefficients and heat transfer parameters, which are important inputs to process design, a full dynamic model of the DCB apparatus is needed. Such a model requires the solution of the partial differential equations describing the component material, momentum and energy balances as a function of time and position along the packed column. While such models exist in the literature (Simo et al. 2008; Farooq and Ruthven 1990; Warmuzinski and Tanczyk 1997) they must be adapted to the particular details of this apparatus, for example to account for the gas residence time and effects of dispersion in the tubes and fittings external to the packed-column. For this

DCB apparatus, the volume of the sections between MPV-1 and BPR-2 have the most effect on the observed gas residence times because in these sections the gas pressure could be up to 1000 kPa, and thus these sections could store up to 10 times their standard volume.

The DCB apparatus provides a rapid procedure for comparing candidate adsorbents for a given gas separation application by allowing the direct measurement of selectivity. An adsorbent's equilibrium selectivity, α_{ij}, for two components in a gas mixture (i is the more adsorbed component and j the less adsorbed component) is defined (for example, Saha et al. 2010):

$$\alpha_{ij} \equiv \left(\frac{x_i}{x_j}\right)\left(\frac{y_j}{y_i}\right). \tag{11}$$

Here x_i is the mole fraction of component i in the adsorbed phase. This quantity can be measured directly using the DCB apparatus by flowing the gas mixture across the adsorbent until equilibrium is reached, and then determining the adsorbed phase mole fractions from the measured $Q^*_{\mathrm{abs},i}/Q^*_{\mathrm{tot}}$. Such measurements are quite difficult to make using static volumetric or gravimetric adsorption systems because a capacity to both stir and sample the vapor phase is required, such as in the system described by Watson et al. (2012). As a consequence of this difficulty, estimates of an adsorbent's selectivity are frequently made on the basis of measured pure fluid capacities. For example, Gu and Lodge (2011) and Jensen et al. (2012) estimated so-called 'inferred' or 'ideal' selectivities, $(\alpha_{ij})_{\mathrm{inf}}$, as in Eq. (12), which are computationally simple to evaluate for equimolar mixtures. These can provide an initial indication of the potential of an adsorbent for a gas separation application; however, the inferred selectivities $(\alpha_{ij})_{\mathrm{inf}}$ computed with Eq. (12) do not account for competition between species for adsorption sites.

$$(\alpha_{ij})_{\mathrm{inf}} = \left(\frac{Q^*_{\mathrm{pure},i}}{Q^*_{\mathrm{pure},j}}\right). \tag{12}$$

More rigorous predictions of mixture selectivity can be made by using, for example, the Ideal Adsorbed Solution theory (IAST) developed by Myers and Prausnitz (1965) although such methods can be expensive in both measurement time and computational effort. Sufficient data must be acquired to regress reliably equilibrium adsorption capacity models for the two pure fluids at the temperature of interest, and then these models must be used iteratively in the evaluation of integrals used to equate spreading pressures. In contrast, the DCB apparatus can be used to readily determine equilibrium adsorption selectivities for a gas mixture with a single measurement, which is no more difficult than a pure fluid adsorption measurement at the same condition.

Table 2 Component uncertainties associated with the dynamic breakthrough apparatus

Component	Uncertainty
MFM [with Eq. (1)]	1.6 % of reading + 0.2 % of full scale
MFC	0.8 % of reading + 0.2 % of full scale
BPR	0.25 % of full scale
QPT	±0.1 kPa
MS	±1 % by mole
T (platinum resistance)	±0.2 K
Mass of adsorbent	±5 mg

4 Quantitative estimation of uncertainty

Table 2 contains a list of the sources of measurement uncertainty associated with the dynamic column apparatus. Of these uncertainty sources, the most significant is the measurement of the difference in mass flows entering and leaving the column. To estimate this quantitatively, it is convenient to define an average difference flow rate, $\overline{\Delta f} \equiv m\,Q^*_{\mathrm{ex,tot}}/(t_{\mathrm{eq}} - t_0)$. Then, with $u(x)$ and $u_r(x)$ denoting the absolute and relative uncertainties of a quantity x, respectively, an error propagation analysis gives:

$$\frac{u(Q^*_{\mathrm{ex,tot}})}{Q^*_{\mathrm{ex,tot}}} \cong \frac{u(\overline{\Delta f})}{\overline{\Delta f}} \tag{13}$$

because $u_r(m) \ll u_r(\overline{\Delta f})$ and $u_r(t_{\mathrm{eq}} - t_0) \ll u_r(\overline{\Delta f})$. From Eq. (10) and the definition of $\overline{\Delta f}$, its value can be calculated from difference in the inlet and effluent flow rates averaged over the time interval $(t_{\mathrm{eq}} - t_0)$

$$\overline{\Delta f} = \langle f - F \rangle \underset{f=\mathrm{const}}{\rightarrow} \overline{\Delta f} = f - \langle F \rangle. \tag{14}$$

Here the angled brackets denote the time average. The second equality holds when the inlet flow to the column was held constant throughout the experiment, as was the case in this work. Thus

$$\frac{u(Q^*_{\mathrm{ex,tot}})}{Q^*_{\mathrm{ex,tot}}} \cong \frac{\sqrt{u(f)^2 + u(\langle F \rangle)^2}}{f - \langle F \rangle}. \tag{15}$$

It is apparent from Eq. (15) that the uncertainty in the derived equilibrium capacity depends on the rate and magnitude of the adsorption. If F changes significantly and quickly (for example when sorption kinetics are fast), the uncertainty in the corresponding $Q^*_{\mathrm{ex,tot}}$ determination will be much lower than if the variation in F is small and/or over a longer period (such as when sorption kinetics are slow). More importantly, the value of $Q^*_{\mathrm{ex,tot}}$ and its uncertainty depend on the choice of t_{eq}, yet a judgement is generally required because f and F approach each other asymptotically as the adsorption process approaches saturation. In general there is a certain critical value t^*_{eq} above which the value

of $Q^*_{ex,tot}$ determined from Eq. (10) is insensitive; however, the larger the value t_{eq} chosen, the greater the value of $u(Q^*_{ex,tot})$. Conversely, a choice of t_{eq} significantly below t^*_{eq} will reduce the value of $u(Q^*_{ex,tot})$ calculated with Eq. (15) but lead to an systematic reduction in the estimate of $Q^*_{ex,tot}$. For this reason, we evaluated $u(Q^*_{ex,tot})$ using values of t_{eq} such that the estimated uncertainty was about (30 to 100) % larger than the change in $Q^*_{ex,tot}$obtained with using t^*_{eq}. In practice, the return of the bed's temperature profile to the initial condition can be used as a guide as to when t^*_{eq} has been reached.

The uncertainty in the component equilibrium adsorption capacities determined with this DCB apparatus can be estimated in a similar way:

$$\frac{u(Q^*_{ex,j})}{Q^*_{ex,j}} \cong \frac{\sqrt{u(f_j)^2 + u(\langle F_j\rangle)^2 + u(y^*_j F_{He})^2}}{f_j - \langle F_j\rangle - y^*_j\langle F_{He}\rangle}. \quad (16)$$

Here, $F_j = y_j F$ is the effluent molar flow of component j and F_{He} is the effluent molar flow of helium. The additional uncertainty associated with the measurement of the gas composition will in general mean that $u(Q^*_{ex,j}) > u(Q^*_{ex,tot})$. However, the y_i are subject to a normalization constraint and thus $u(Q^*_{ex,j})$ will depend upon the number of species in the feed gas and in the case of a pure fluid adsorbate, the uncertainties calculated using Eqs. (15) and (16) are equal.

5 Results and discussion

The dynamic column breakthrough apparatus was used to test and compare two zeolite adsorbents for the separation of $CH_4 + N_2$ gas mixtures that have been studied by others: mordenite and 13X. Pure fluid adsorption capacities were first measured at 301.9 K. Pure fluid measurements of the adsorbent with the largest capacities at this temperature (13X) were then conducted at 229.2 K. In addition, measurements with a gas mixture were conducted to determine whether the adsorbents' equilibrium selectivities were comparable with those inferred from the pure fluid measurements. The measured values of Q^*_{ex,CH_4} and Q^*_{ex,N_2} for the pure fluids are listed in Tables 3 and 4 for mordenite and 13X, respectively. The measured values of Q^*_{ex,CH_4} and Q^*_{ex,N_2} for the $CH_4 + N_2$ mixtures on both zeolites are listed in Table 5. Absolute adsorption capacities, $Q^*_{abs,i}$, for pure fluids and the $CH_4 + N_2$ mixtures are also listed in Tables 3–5. At the measurement conditions in this study the difference between absolute and excess adsorption capacities was small with$(Q^*_{abs,i} - Q^*_{ex,i})/Q^*_{ex,i} \le 0.02$.

Dynamic data acquired during a typical pure fluid experiment are shown in Fig. 2; analysis of the data acquired at each fixed pressure and temperature with Eq. (10) leads to the pure fluid adsorption capacities listed in Tables 3 and 4.

Table 3 Equilibrium excess ($Q^*_{ex,i}$) and absolute ($Q^*_{abs,i}$) adsorption capacities of N_2 and CH_4 on H^+-mordenite at 301.9 K measured on the DCB apparatus with pure fluids. The uncertainty $u(Q^*_{ex,i})$ in the adsorption capacity measurement is also reported

Adsorbate, i	P (kPa)	$Q^*_{ex,i}$ (mmol g^{-1})	$u(Q^*_{ex,i})$ (mmol g^{-1})	$Q^*_{abs,i}$ (mmol g^{-1})
N_2	106.2	0.17	0.04	0.17
N_2	276.0	0.37	0.04	0.37
N_2	447.8	0.54	0.05	0.54
N_2	620.1	0.68	0.06	0.69
N_2	792.0	0.79	0.06	0.80
CH_4	104.0	0.51	0.06	0.51
CH_4	275.8	0.93	0.06	0.93
CH_4	447.9	1.18	0.07	1.19
CH_4	619.8	1.33	0.07	1.35
CH_4	791.7	1.46	0.07	1.48

Table 4 Equilibrium excess ($Q^*_{ex,i}$) and absolute ($Q^*_{abs,i}$) adsorption capacities of N_2 and CH_4 on zeolite 13X at 301.9 K and 229.2 K measured on the DCB apparatus with pure fluids. The uncertainty $u(Q^*_{ex,i})$ in the adsorption capacity measurement is also reported

Adsorbate, i	T (K)	P (kPa)	$Q^*_{ex,i}$ (mmol g^{-1})	$u(Q^*_{ex,i})$ (mmol g^{-1})	$Q^*_{abs,i}$ (mmol g^{-1})
N_2	301.9	106.8	0.29	0.05	0.29
N_2	301.9	792.9	1.34	0.10	1.36
N_2	229.2	792.6	3.28	0.12	3.33
CH_4	301.9	104.8	0.50	0.06	0.50
CH_4	301.9	792.5	2.09	0.14	2.13
CH_4	229.2	792.3	3.89	0.19	3.97

The pure fluid equilibrium capacities for mordenite measured on the DCB apparatus are compared in Fig. 4 with the volumetric adsorption measurements reported by Delgado et al. (2006a) and with those made in our own laboratory by Jensen et al. (2012). The latter authors measured the equilibrium adsorption capacity of the same H^+-mordenite sample studied in this work at 303.15 K and pressures from 5 to 119.5 kPa. Delgado et al. (2006a) used a volumetric system to obtain equilibrium adsorption data for CH_4 and N_2 on H^+-mordenite synthesized from ion-exchanged Na^+ mordenite supplied by CU Chemie Uetikon AG. Their experiments were performed at 279, 293, and 308 K at pressures to 2000 kPa. From their data, Delgado et al. (2006a) determined parameters for Toth models of mordenite's N_2 and CH_4 adsorption capacities over this range of conditions. The predictions of Delgado et al.'s Toth models are shown in Fig. 4(a) at the experimental conditions corresponding to those measured in this work. In Fig. 4(a) the data of Jensen et al. (2012) were corrected to equivalent capacities

Table 5 Excess ($Q^*_{ex,i}$) and absolute ($Q^*_{abs,i}$) adsorption capacities determined from the DCB measurements with $CH_4 + N_2$ mixtures and predicted with the Ideal Adsorbed Solution Theory ($Q_{IAST,i}$) using pure fluid Toth model parameters for mordenite and 13X reported by Delgado et al. (2006a) and Cavenati et al. (2004), respectively. Also listed are the adsorption selectivities (α_{CH_4,N_2}) of CH_4 over N_2 on mordenite and 13X measured with $CH_4 + N_2$ mixtures on the DCB $(\alpha_{CH_4,N_2})_{meas}$ and predicted with the IAST models $(\alpha_{CH_4,N_2})_{IAST}$. The average uncertainties in $(\alpha_{CH_4,N_2})_{meas}$ for mordenite and 13X are ±0.4 and ±0.2, respectively

y_{CH_4}	T (K)	P (kPa)	Q^*_{ex,CH_4} (mmol g^{-1})	Q^*_{ex,N_2} (mmol g^{-1})	$u(Q^*_{ex,total})$ (mmol g^{-1})	Q^*_{abs,CH_4} (mmol g^{-1})	Q^*_{abs,N_2} (mmol g^{-1})	Q_{IAST,CH_4} (mmol g^{-1})	Q_{IAST,N_2} (mmol g^{-1})	$(\alpha_{CH_4,N_2})_{meas}$	$(\alpha_{CH_4,N_2})_{IAST}$
H^+-mordenite											
0.471	301.9	105.1	0.26	0.09	0.06	0.26	0.09	0.30	0.08	3.43	3.88
0.503	301.9	275.8	0.57	0.15	0.06	0.57	0.15	0.61	0.16	3.65	3.93
0.500	301.9	447.9	0.75	0.21	0.08	0.76	0.21	0.81	0.21	3.55	3.95
0.495	301.9	620.0	0.87	0.26	0.08	0.88	0.26	0.96	0.24	3.46	3.98
0.471	301.9	791.8	0.92	0.31	0.08	0.93	0.32	1.06	0.27	3.30	3.98
13X											
0.502	301.9	106.0	0.25	0.14	0.06	0.25	0.14	0.30	0.13	1.75	2.32
0.497	301.9	792.9	1.18	0.59	0.15	1.20	0.60	1.40	0.60	2.03	2.28
0.497	229.2	792.8	2.56	1.12	0.29	2.61	1.15	3.35	1.65	2.31	2.03

at 301.9 K using their reported enthalpy of adsorption. The deviations of our data and those of Jensen et al. (2012) from the predictions of the Toth models developed by Delgado et al. (2006a) are shown in Fig. 4(b).

The N_2 equilibrium capacities measured with the DCB apparatus are in excellent agreement with those predicted using the Toth model from Delgado et al. (2006a), with all the deviations being within the estimated experimental uncertainty of the dynamic measurements. The deviations of the measured CH_4 equilibrium capacities from the model are slightly larger, and are about twice the estimated uncertainty of our data. Unfortunately, Delgado et al. (2006a) did not report their actual data or associated uncertainties, and only reported the parameters of the Toth models fit to their data. Thus it is not possible to determine whether the deviations from the Toth model are smaller than the combined uncertainties of the data and the model. The consistency of the DCB data with those of Jensen et al. (2012) for both the CH_4 and N_2 equilibrium capacities of mordenite is within the experimental uncertainty of this work.

In Fig. 5 we compare the equilibrium N_2 and CH_4 capacities of 13X measured for pure fluids on the DCB apparatus to the adsorption capacities calculated from the Toth model parameters published by Cavenati et al. (2004). Cavenati et al. measured the adsorption capacities of CH_4 and N_2 on a 13X sample from CECA (France) at 298, 308, and 323 K and pressures to 5000 kPa using a static volumetric adsorption apparatus. At 301.9 K the capacities measured with the DCB apparatus at pressures near 105 kPa are consistent with the results of Cavenati et al. (2004) within the experimental uncertainty. At 793 kPa, the N_2 and CH_4 capacities measured with the DCB apparatus deviate from the Toth model predictions by 1.2 and 2.7 times the experimen-

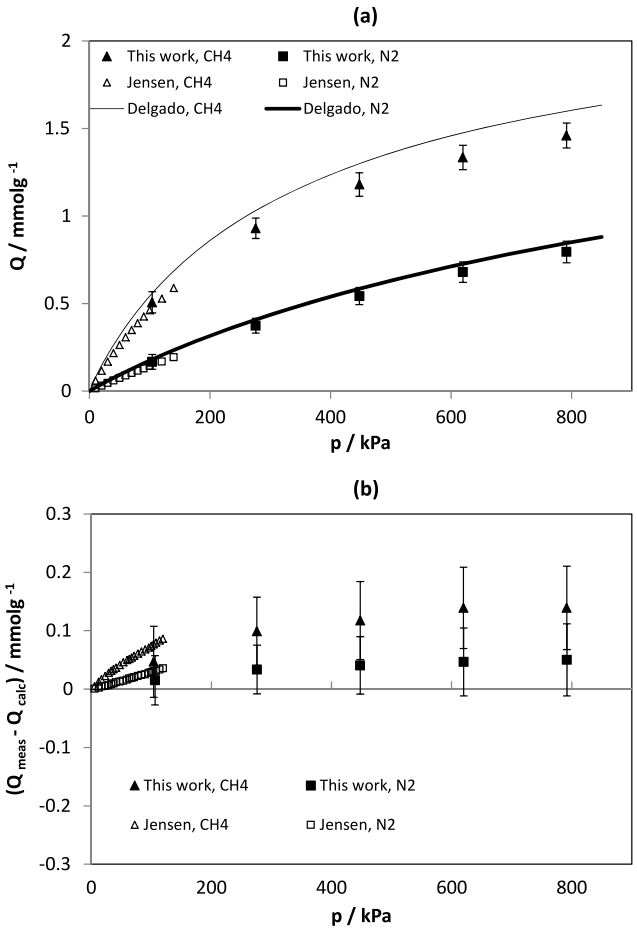

Fig. 4 Adsorption capacity of CH_4 and N_2 on mordenite at 302 K measured with pure fluids using the DCB apparatus. (**a**) Equilibrium capacities measured in this work and by Jensen et al. (2012) are shown together with capacities calculated using the Toth isotherm parameters reported by Delgado et al. (2006a). (**b**) Deviations between the measured capacities and those calculated using the Toth isotherm models

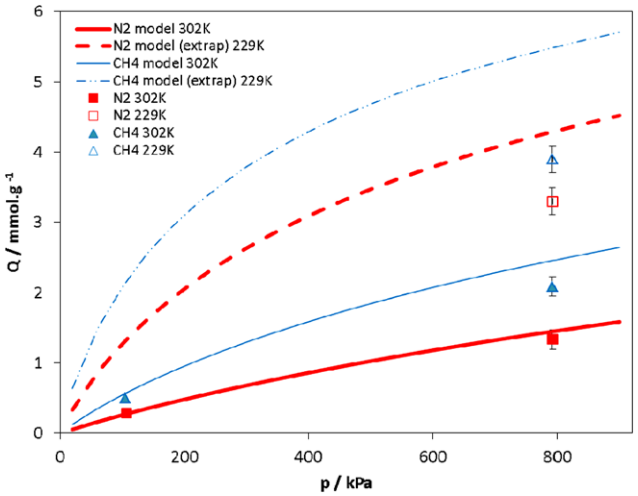

Fig. 5 Adsorption capacity of CH_4 and N_2 on 13X at 302 K and 229 K measured with pure fluids using the DCB apparatus. The data points were measured in this work. Toth parameters from Cavenati et al. (2004) were used to calculate the model curves: the *dashed curves* correspond to an extrapolation of the models, which were regressed to data measured in the range 298 K to 323 K

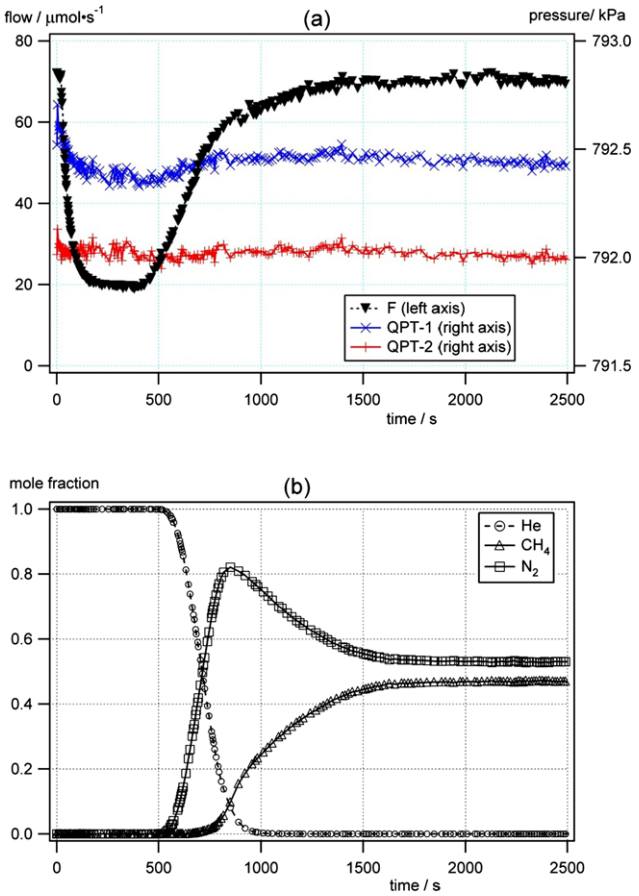

Fig. 6 Dynamic adsorption of $0.47CH_4 + 0.53N_2$ on mordenite at 792 kPa, 301.9 K. (**a**) Column effluent flow rate (*left axis*) and pressures at each end of column (*right axis*). (**b**) Effluent mole fraction compositions

tal uncertainty, respectively. Again it is difficult to assess the magnitude of these deviations because Cavenati et al. (2004) did not estimate the uncertainty of their data or report the average deviation of their data from the best-fit models. Nevertheless, the level of agreement observed between data sets is generally as good as can be expected for experimental measurements of adsorption using different instruments, techniques and adsorbent samples. Furthermore, it is likely that some of these differences are due to the precise nature of the adsorbent samples and their history prior to measurement.

The pure fluid DCB measurements at 301.9 K indicated that 13X has a larger equilibrium capacity for both CH_4 and N_2 than mordenite. Extrapolating the Toth adsorption capacity models of Cavenati et al. (2004) for 13X to 229.2 K suggests that the CH_4 and N_2 capacities would increase from their values at 301.9 K by a factor of 2.2 and 2.9, respectively at a pressure of 793 kPa. Such increases could be helpful in reducing the necessary size of a 13X PSA tower used in a gas separation process. To test this prediction, dynamic adsorption measurements were conducted with the 13X zeolite at 229.2 K and 793 kPa. In Fig. 5, the results of these low temperature pure fluid measurements are shown together with the capacities predicted using the extrapolated Toth models. The ratios of the measured values of $Q^*_{\mathrm{abs,CH_4}}$ and $Q^*_{\mathrm{abs,N_2}}$ at the two temperatures were 1.9 and 2.5, respectively. For both fluids the actual increases in capacity are 20 % below the increases predicted with the extrapolated models, while the fractional differences between the measured and predicted capacities were −30 % for N_2 and −40 % for CH_4. This example demonstrates the dangers of extrapolating adsorption capacity models down in temperature, in this case about 70 K below the lowest temperature measurements of Cavenati et al. (2004) As a corollary, it demonstrates the importance of low temperature adsorption capacity measurements if the potential advantages of operating a PSA process at temperatures accessible in cryogenic gas plants are to be assessed reliably.

Selectivity is the other key adsorbent property that needs to be quantified for gas separation applications and, while estimates from pure fluid measurements are possible, measurements with mixtures are crucial if selectivity is to be determined accurately. Figure 6 shows characteristic dynamic data for the effluent gas flow and composition for the adsorption of a $0.47CH_4 + 0.53N_2$ gas mixture on mordenite at 793 kPa and 301.9 K. The slightly increased noise apparent in the effluent flow rate in comparison with that shown in Fig. 2 is due to the action of the BPR, which maintained the column at the higher pressure (the time series for the pressures at each end of the column are also shown plotted on the right axis of Fig. 6(a)). Analysis of the dynamic mixture data such as those shown in Fig. 6 using Eq. (9) enable component and total equilibrium adsorption capacities to be determined. Figure 7 shows these capacities for the set of $zCH_4 +$

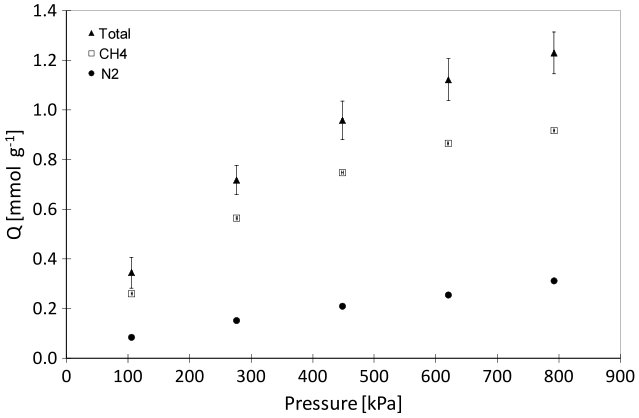

Fig. 7 Adsorption capacities for $z\mathrm{CH_4} + (1-z)\mathrm{N_2}$ gas mixtures, with $z = 0.49 \pm 0.02$, in equilibrium with mordenite at 301.9 K

$(1-z)\mathrm{N_2}$ mixtures, with $z = 0.49 \pm 0.02$, in equilibrium with mordenite at 301.9 K as a function of mixture pressure.

The total and component adsorption capacities for $\mathrm{CH_4}$ and $\mathrm{N_2}$ from these gas mixtures are listed in Table 5. Also shown are the predicted adsorbed capacities for each component calculated using the IAST, which was implemented using the algorithm of Valenzuela and Myers (1989) together with the pure fluid Toth isotherm parameters of Delgado et al. (2006a) for mordenite and Cavenati et al. (2004) for 13X. No parameters were adjusted within the IAST models. In most cases, the predictions of the adsorbed $\mathrm{CH_4}$ and $\mathrm{N_2}$ capacities are consistent with the values measured by the DCB apparatus within the experimental uncertainties. The largest difference between the measured adsorption capacity and the predictions of the IAST model was in the adsorption of $\mathrm{CH_4} + \mathrm{N_2}$ on 13X at 229.2 K. However, the discrepancy of about 26 % in $Q^*_{\mathrm{ex,tot}}$ in this case is due principally to the low-temperature extrapolation of the models used for pure fluid capacities (see Fig. 5) rather than of the IAST itself. This emphasizes how the predictions of the IAST model are sensitive to the uncertainties of the pure fluid adsorption isotherms which increase significantly when models are extrapolated beyond the data to which they were regressed.

The selectivities, $(\alpha_{\mathrm{CH_4,N_2}})_{\mathrm{meas}}$, calculated using Eq. (11) for mordenite and 13X are presented in Table 5 along with the selectivities predicted from the IAST models. The measured values of $\alpha_{\mathrm{CH_4,N_2}}$ were approximately constant with pressure and temperature for both zeolites; the observed variations were comparable with the estimated uncertainty in the measured mixture selectivity. For mordenite at 301.9 K $\alpha_{\mathrm{CH_4,N_2}}$ had an average value of 3.5 ± 0.1, while for 13X the average was 2.0 ± 0.3. The selectivities estimated using the IAST models based on the pure fluid isotherms were 7–20 % larger for the mordenite and up to 32 % larger for the 13X. These deviations again reflect the propagation of pure fluid adsorption isotherm uncertainties in the calculation of predicted selectivities and underscore the importance of conducting mixture measurements when screening and assessing adsorbents for gas separation applications.

6 Conclusions

In this work a column breakthrough apparatus capable of multi-component adsorption measurements over a wide range of pressure and temperature was described. We also presented a detailed description of the experimental procedure and the methods of analyzing the data to determine equilibrium capacities with quantitative uncertainties. Adsorption capacity data for the mordenite and 13X zeolites were presented to demonstrate the apparatus can be used to: (1) generate equilibrium isotherms for pure gases and mixtures, (2) rapidly compare adsorbents for a gas separation application based on capacity and selectivity, and (3) test adsorbents with mixtures at low temperatures and high pressures. We also demonstrated that a reliance on pure fluid measurements to estimate equilibrium selectivities can result in significant errors.

The mordenite and 13X zeolites both showed preferential adsorption of $\mathrm{CH_4}$ over $\mathrm{N_2}$. At low temperatures the equilibrium capacity and selectivity of the 13X increased significantly. However, for both the 13X and mordenite zeolites the equilibrium capacities and selectivities are unlikely to be sufficient for a large scale industrial gas separation process.

Acknowledgements The research was funded by Chevron Energy Technology Company, the Western Australian Energy Research Alliance and the Australian Research Council (Project LP0776928). One of us (PSH) also received scholarships from the Australia China Natural Gas Partnership Fund and the Australian Petroleum Production and Exploration Association. We thank Craig Grimm for helping to construct the apparatus as well as Guillaume Watson, Brendan Graham and Thomas Saleman for their contributions to the research, and Mike Johns and Brent Young for carefully reading the manuscript. We are grateful to TOSOH Corporation and Shanghai MLC for supplying the zeolites studied in this work.

References

Al-Muhtaseb, S.A.: Adsorption and desorption equilibria of nitrogen, methane, ethane, and ethylene on date-pit activated carbon. J. Chem. Eng. Data **55**(1), 313–319 (2010)

American Energies Pipeline, LLC: Improve Gas Quality—Nitrogen Rejection Unit (2009). http://www.nitrogenrejectionunit.com/facts.html. Accessed 29/10/2010 2010

Assael, M.J., Trusler, J.P.M., Tsolakis, T.F.: Thermophysical Properties OF Fluids: An Introduction to Their Prediction. World Scientific, Singapore (1996)

Broom, D.P.: Hydrogen Storage Materials: The Characterisation of Their Storage Properties. Springer, London (2011)

Campbell, J.M.: Gas conditioning and processing/by John M. Campbell; With a collaboration on chapter 11 by R.N. Maddox. vol. Accessed from http://nla.gov.au/nla.cat-vn2360714. Campbell Petroleum Series, Norman, Okla. (1974)

Casas, N., Schell, J., Pini, R., Mazzotti, M.: Fixed bed adsorption of CO_2/H_2 mixtures on activated carbon: experiments and modeling. Adsorption (2012)

Cavenati, S., Grande, C.A., Rodrigues, A.E.: Adsorption equilibrium of methane, carbon dioxide, and nitrogen on zeolite 13X at high pressures. J. Chem. Eng. Data **49**(4), 1095–1101 (2004)

Delgado, J.A., Uguina, M.A., Gomez, J.M., Ortega, L.: Adsorption equilibrium of carbon dioxide, methane and nitrogen onto Na- and H-mordenite at high pressures. Sep. Purif. Technol. **48**(3), 223–228 (2006a)

Delgado, J.A., Uguina, M.A., Sotelo, J.L., Ruiz, B.: Modelling of the fixed-bed adsorption of methane/nitrogen mixtures on silicalite pellets. Sep. Purif. Technol. **50**(2), 192–203 (2006b)

Do, D.D.: Adsorption Analysis: Equilibria and Kinetics. Imperial College Press, London (1998)

Farooq, S., Ruthven, D.M.: Heat effects in adsorption column dynamics. 2. Experimental validation of the one-dimensional model. Ind. Eng. Chem. Res. **29**(6), 1084–1090 (1990)

Grande, C.A., Silva, V., Gigola, C., Rodrigues, A.E.: Adsorption of propane and propylene onto carbon molecular sieve. Carbon **41**(13), 2533–2545 (2003)

Gu, Y., Lodge, T.P.: Synthesis and gas separation performance of triblock copolymer ion gels with a polymerized ionic liquid midblock. Macromolecules **44**(7), 1732–1736 (2011)

Guntuka, S., Farooq, S., Rajendran, A.: A- and B-site substituted lanthanum cobaltite perovskite as high temperature oxygen sorbent. 2. Column dynamics study. Ind. Eng. Chem. Res. **47**(1), 163–170 (2008)

Habgood, H.W.: The kinetics of molecular sieve action—sorption of nitrogen-methane mixtures by linde molecular sieve 4A. Can. J. Chem.-Rev. Can. Chim. **36**(10), 1384–1397 (1958)

Hofman, P.S.: Dynamic mixture measurements of commercial adsorbents for evaluating $N_2 + CH_4$ separations by pressure swing adsorption for liquified natural gas production. PhD Thesis, The University of Western Australia (2012)

Jensen, N.K., Rufford, T.E., Watson, G., Zhang, D.K., Chan, K.I., May, E.F.: Screening of several zeolites for gas separation applications involving methane, nitrogen, and carbon dioxide. J. Chem. Eng. Data **57**(1), 106–113 (2012)

Karger, J., Ruthven, D.M.: Diffusion in Zeolites and Other Microporous Solids. Wiley, New York (1992)

Keller, J.U., Staudt, R.: Gas Adsorption Equilibria: Experimental Methods and Adsorptive Isotherms. Springer, Boston (2010)

Kidnay, A.J., Parrish, W.R.: Fundamentals of Natural Gas Processing. CRC Press, Boca Raton (2006)

Kunz, O., Klimeck, R., Wagner, W., Jaeschke, M.: The GERG-2004 Wide-Range Reference Equation of State for Natural Gases and Other Mixtures. GERG Technical Monograph. In. Fortschr.-Ber. VDI, VDI-Verlag, Düsseldorf (Germany) (2006)

Kuznicki, S.M., Bell, V.A., Nair, S., Hillhouse, H.W., Jacubinas, R.M., Braunbarth, C.M., Toby, B.H., Tsapatsis, M.: A titanosilicate molecular sieve with adjustable pores for size-selective adsorption of molecules. Nature **412**(6848), 720–724 (2001)

LabVIEW. In. National Instruments (2007)

Lemmon, E.W., Huber, M.L., McLinden, M.O.: REFPROP—reference fluid thermodynamic and transport properties. NIST Standard Reference Database 23. In. (2007)

Lopes, F.V.S., Grande, C.A., Rodrigues, A.E.: Activated carbon for hydrogen purification by pressure swing adsorption: Multicomponent breakthrough curves and PSA performance. Chem. Eng. Sci. **66**(3), 303–317 (2011)

Malbrunot, P., Vidal, D., Vermesse, J., Chahine, R., Bose, T.K.: Adsorbent helium density measurement and its effect on adsorption isotherms at high pressure. Langmuir **13**, 539–544 (1997)

Malek, A., Farooq, S.: Determination of equilibrium isotherms using dynamic column breakthrough and constant flow equilibrium desorption. J. Chem. Eng. Data **41**(1), 25–32 (1996)

Mitariten, M.: Nitrogen removal from natural gas with the molecular gate adsorption process. Paper presented at the Gas Processors Association (2009)

Mulgundmath, V.P., Jones, R.A., Tezel, F.H., Thibault, J.: Fixed bed adsorption for the removal of carbon dioxide from nitrogen: Breakthrough behavior and modelling for heat and mass transfer. Sep. Purif. Technol. **85**, 17–27 (2012)

Myers, A.L., Prausnitz, J.M.: Thermodynamics of mixed-gas adsorption. AIChE J. **11**, 121–127 (1965)

Rajendran, A., Kariwala, V., Farooq, S.: Correction procedures for extra-column effects in dynamic column breakthrough experiments. Chem. Eng. Sci. **63**(10), 2696–2706 (2008)

Ross, S., Olivier, J.P.: On Physical Adsorption. Interscience, New York (1964)

Rouquerol, F., Rouquerol, J., Sing, K.: Adsorption by Powders and Porous Solids: Principles, Methodology and Applications. Academic Press, New York (1999)

Ruthven, D.M.: Principles of Adsorption and Adsorption Processes. Wiley, New York (1984)

Ruthven, D.M.: Molecular sieve separations. Chem. Ing. Tech. **83**(1–2), 44–52 (2011)

Saha, D., Bao, Z., Jia, F., Deng, S.: Adsorption of CO2, CH4, N2O, and N2 on MOF-5, MOF-177, and zeolite 5A. Environ. Sci. Technol. **44**(5), 1820–1826 (2010)

Sep-Pro Systems Inc.: Nitrogen Rejection Units (2009). http://www.sepprosystems.com/Nitrogen_Rejection_Units.html

Simo, M., Brown, C.J., Hlavacek, V.: Simulation of pressure swing adsorption in fuel ethanol production process. Comput. Chem. Eng. **32**(7), 1635–1649 (2008)

Sircar, S.: Pressure swing adsorption. Ind. Eng. Chem. Res. **41**(6), 1389–1392 (2002)

Sircar, S.: Basic research needs for design of adsorptive gas separation processes. Ind. Eng. Chem. Res. **45**(16), 5435–5448 (2006)

Sircar, S.: Recent developments in macroscopic measurement of multicomponent gas adsorption equilibria, kinetics, and heats. Ind. Eng. Chem. Res. **46**(10), 2917–2927 (2007)

Sudibandriyo, M., Pan, Z., Fitzgerald, J.E., Robinson, R.L., Gasem, K.A.M.: Adsorption of methane, nitrogen, carbon dioxide, and their binary mixtures on dry activated carbon at 318.2 K and pressures up to 13.6 MPa. Langmuir **19**(13), 5323–5331 (2003)

Tezel, F.H., Tezel, H.O., Ruthven, D.M.: Determination of pure and binary isotherms for nitrogen and krypton. J. Colloid Interface Sci. **149**(1), 197–207 (1992)

Tucker Gas Processing Equipment Inc.: Nitrogen Rejection (2011). http://www.tuckergas.com/nrupg03.htm

Valenzuela, D.P., Myers, A.L.: Adsorption Equilibrium Data Handbook. Prentice Hall Advanced Reference Series. Prentice Hall, Englewood Cliffs (1989)

Warmuzinski, K., Tanczyk, M.: Multicomponent pressure swing adsorption. 1. Modelling of large-scale PSA installations. Chem. Eng. Process. **36**(2), 89–99 (1997)

Watson, G.C., Jensen, N.K., Rufford, T.E., Chan, K.I., May, E.F.: Volumetric adsorption measurements of N_2, CO_2, CH_4, and a $CO_2 + CH_4$ mixture on a natural chabazite from 5 to 3000 kPa. J. Chem. Eng. Data **57**(1), 93–101 (2012)

Won, W., Lee, S., Lee, K.-S.: Modeling and parameter estimation for a fixed-bed adsorption process for CO_2 capture using zeolite 13X. Sep. Purif. Technol. **85**, 120–129 (2012)

Yang, R.T.: Gas Separation by Adsorption Processes. Butterworths, Boston (1987)

Young, D.M., Crowell, A.D.: Physical Adsorption of Gases. Butterworths, London (1962)